Biochemical and Biophysical Research Communications xxx (2017) 1–7

Contents lists available at ScienceDirect

Biochemical and Biophysical Research Communications

journal homepage: www.elsevier.com/locate/ybbrc

Interaction assessments of the first S-adenosylmethionine competitive inhibitor and the essential interacting partner methylosome protein 50 with protein arginine methyltransferase 5 by combined computational methods

Kongkai Zhu [a, 1], Cheng-Shi Jiang [a, 1], Junchi Hu [b, c, 1], Xigong Liu [a], Xue Yan [a], Hongrui Tao [a], Cheng Luo [b, **], Hua Zhang [a, *]

[a] School of Biological Science and Technology, University of Jinan, Jinan 250022, China
[b] Drug Discovery and Design Center, State Key Laboratory of Drug Research, Shanghai Institute of Materia Medica, Chinese Academy of Sciences, Shanghai 201203, China
[c] University of Chinese Academy of Sciences, Beijing 100049, China

ARTICLE INFO

Article history:
Received 4 November 2017
Accepted 13 November 2017
Available online xxx

Keywords:
PRMT5 SAM competitive inhibitor
Molecular docking
Molecular dynamics simulation
Molecular mechanics/Poisson-Boltzmann surface area
PRMT5:MEP50 interaction

ABSTRACT

Protein arginine methyltransferase 5 (PRMT5) is the most promising anticancer target in PRMT family. In this study, based on the first S-adenosylmethionine (SAM) competitive small molecule inhibitor (**17**, compound number is from original paper) of PRMT5 reported in our recent paper, we determined the molecular mechanism of **17** interacting with PRMT5 by computational methods. Previously reported **CMP5** was also thought of as a SAM competitive inhibitor of PRMT5, but the direct inhibition activity against PRMT5 at enzymatic level was not provided. Therefore, we tested the half-maximal inhibitory concentration (IC_{50}) of **CMP5** against PRMT5 at enzymatic level for the purpose of summarizing the interaction characteristics of SAM binding site inhibitors with PRMT5. Additionally, as the essential interacting partner of PRMT5, the binding attributes of the WD-repeat-containing protein MEP50 (methylosome protein 50) was investigated, and nine key residues that contribute most to PRMT5:MEP50 interaction were identified. These results could be helpful in discovering new potent and specific inhibitors of PRMT5, as well as in designing mutant residue assay to modulate the catalytic activity of PRMT5.

1. Introduction

As one of the common cellular posttranslational modifications in eukaryotic organisms [1,2], arginine methylation mediated by protein arginine methyltransferases (PRMTs) plays crucial roles in many cellular processes, *e.g.* gene transcription, RNA processing, DNA repair, etc [3,4]. PRMTs could methylate many different protein substrates in nucleus and cytoplasm, which links up well with its important and diverse function. The PRMT family consists of nine members (PRMT1–9) in human cells [5], and they all use SAM as the methyl donor while the *N*-atoms in the sidechain of arginine residues as the methyl acceptor during catalysis. According to the states of methylated arginine [monomethylarginine (MMA), asymmetric dimethylarginine (ADMA), and symmetric dimethylarginine (SDMA)], PRMTs can be further classified into three types: type I, II and III. PRMT1, -2, -3, -4, -6 and -8 belong to type I, which could convert arginine to MMA and further to ADMA [5,6]. PRMT5 [7] and −9 [8] appertain to type II which could generate MMA and SDMA, while PRMT7 is the only type III PRMT enzyme that solely produces MMA [9].

Numerous studies [10–13] have indicated the vital roles of PRMT5 misregulation in disease development, notably in cancer. As a consequence, mounting efforts [12,14–18] have been made to develop PRMT5 inhibitors (Chart 1) considering its potential therapeutic prospect in cancer therapy. Although inhibitors of every PRMT member are reported [2], only one PRMT5 inhibitor (**GSK-3326595**) has been put into clinical trials. Thus, PRMT5 draws more

* Corresponding author.
** Corresponding author.
E-mail addresses: cluo@simm.ac.cn (C. Luo), bio_zhangh@ujn.edu.cn (H. Zhang).
[1] These authors contributed equally.

https://doi.org/10.1016/j.bbrc.2017.11.089
0006-291X/

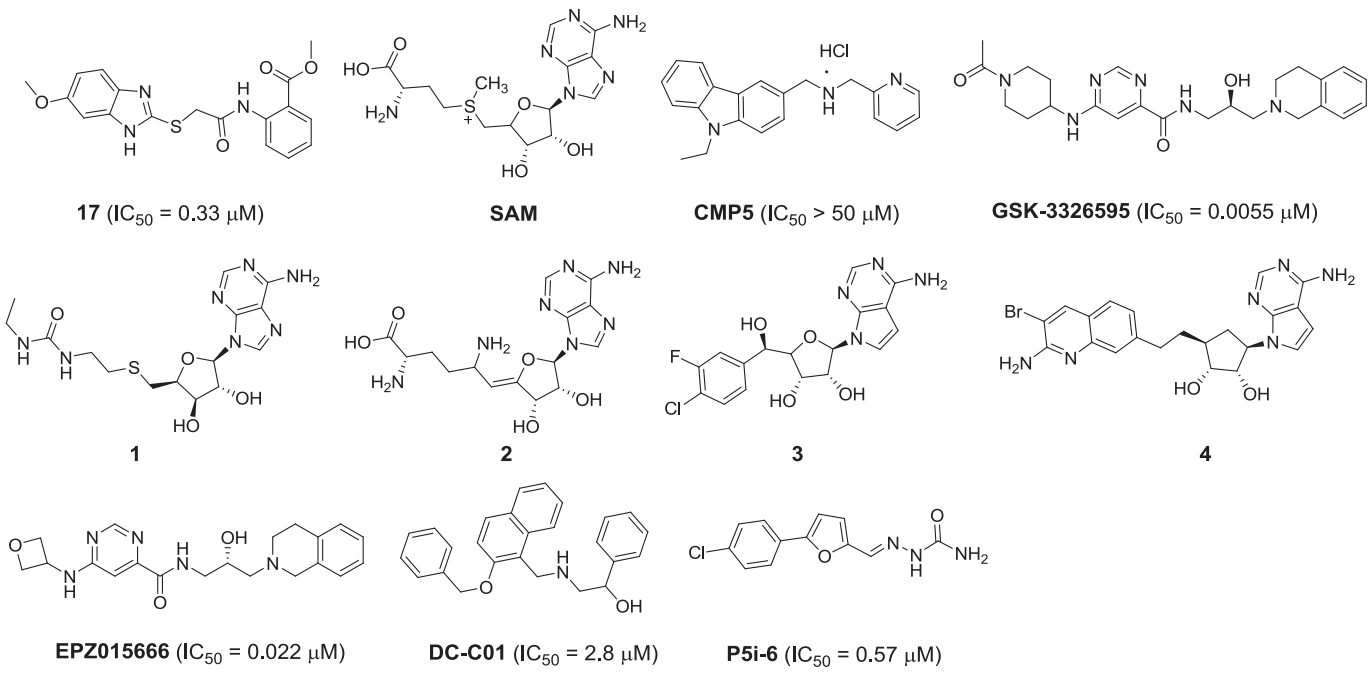

Chart 1. Previously reported PRMT5 inhibitors.

attention among PRMTs and becomes the most promising target for anticancer therapy. Two sites (SAM binding site, substrate binding site) on PRMT5 that can be occupied, thus the reported PRMT5 inhibitors (Chart 1) can be classified into SAM binding site (compound **1**–**4** [18–21], **17** [14]) and substrate binding site (**EPZ015666** [17]) inhibitors. However, the binding sites of some inhibitors (**CMP5** [12], **DC-C01** [15] and **P5i-6** [16]) have not been verified. According to the structure characteristics, previously reported PRMT5 inhibitors can be grouped into SAM analogues (**1**–**4**), which have poor selectivity and druggability, and non-SAM analogues.

Compound **17** is the first SAM competitive inhibitor of PRMT5 reported in our recent paper with an IC_{50} of 0.33 μM [14]. To probe its binding mode with PRMT5, we tried to obtain the complex crystal structure but failed. Therefore, as an alternative method, we used molecular docking and molecular dynamics (MD) simulation to investigate the interactions between **17** and PRMT5 in the present study. **CMP5** was also reported to be a SAM binding site inhibitor of PRMT5 [12], but its direct inhibition activity against PRMT5 at enzymatic level was not tested. As the aim of this study is to summarize the interaction characteristics of SAM binding site inhibitors with PRMT5 by computational methods, it is necessary to acquire the IC_{50} of **CMP5**. We thus synthesized this compound and used radioactive methylation assay to test its activity against PRMT5. Our result showed that the IC_{50} value of **CMP5** was above 50 μM, which indicated that PRMT5 is not the direct target of **CMP5**. Accordingly, its binding interaction with PRMT5 was not investigated in the current work.

Our simulation results showed that **17** displayed a binding mode similar to SAM and formed quite stable hydrogen bonds and hydrophobic interactions with PRMT5, with the binding free energy of −27.27 kcal/mol. In addition, by analyzing the MD trajectories of SAM-PRMT5:MEP50 and SAM-PRMT5 models, regions responsible for the interaction between PRMT5 and MEP50 were localized. Further investigation identified nine key residues that contributed most to PRMT5:MEP50 interaction, and this findings were further validated by fragment docking and direct coupling analysis (FdDCA) method.

2. Material and methods

2.1. Molecular docking

The coordinates of the crystal structures of PRMT5 with SAM analogue (A9145C), MEP50 and H4 peptide were retrieved from the PDB (accession 4GQB [19]). As part of important residues (208–211 and 246–247) of MEP50 in this crystal structure was not determined, we used the coordinate of MEP50 from another PDB (accession 4X60 [17]) which contains the relatively entire MEP50 (sequence: Leu19–Pro328). The protein structure of PRMT5:MEP50 was manually constructed by combining PRMT5 (sequence: R13–Leu637) and MEP50 from the two crystal structures. Molecular docking was performed to obtain the binding mode of **17** to PRMT5:MEP50 with Glide 6.7 (grid-based ligand docking with energetics) program [22,23]. The protein structure was prepared using the Protein Preparation Wizard Workflow provided in the Maestro graphical user interface of the Schrödinger program suite, and the default settings were used. Residues within 15 Å around A9145C in PRMT5 were defined as binding sites at which the docking grids were created. The default settings were adopted for the cutoff, neutralization, scaling and dimension of the binding pocket. Compound **17** and the methyl donor SAM were prepared by LigPrep and the default settings were adopted. Then the extra precision (XP) mode was used to dock **17** and SAM into the defined binding site without constraint. Finally, the **17**-PRMT5:MEP50 and SAM-PRMT5:MEP50 complex models were obtained, respectively. The SAM-PRMT5 model was constructed from SAM-PRMT5:MEP50 complex with manual deletion of MEP50.

2.2. Molecular dynamics simulation

100 ns MD simulations were performed on **17**-PRMT5:MEP50, SAM-PRMT5:MEP50 and SAM:PRMT5 models. The protonation states of ionizable residues of each model were determined using the H++ program [24]. Each complex model was surrounded by a periodic box of transferable intermolecular potential 3P water

Please cite this article in press as: K. Zhu, et al., Interaction assessments of the first S-adenosylmethionine competitive inhibitor and the essential interacting partner methylosome protein 50 with protein arginine methyltransferase 5 by combined computational methods, Biochemical and Biophysical Research Communications (2017), https://doi.org/10.1016/j.bbrc.2017.11.089

molecules that extended 10.0 Å from the protein atoms. Counterions were added to neutralize the simulation system. Molecular dynamics simulations were performed using the AMBER 14.0 package [25] with isothermal-isobaric (NPT) ensemble and periodic boundary conditions. The Amber14SB force field and the general Amber force field (GAFF) [26] were used for protein and small molecules respectively. The charges and force field parameters of SAM and **17** that were not existent in GAFF were derived by antechamber [26,27]. During MD simulations, all bonds involving hydrogen atoms were constrained with the SHAKE algorithm [28], and an integration step of 2 fs was used. Electrostatic interactions were calculated using the particle-mesh Ewald method [29]. The nonbonded cutoff was set to 10 Å, and the nonbonded pairs were updated every 25 steps. Each simulation was coupled to a 300 K thermal bath at 1 bar pressure by applying the algorithm of Berendsen et al. [30].

2.3. MM-PBSA calculations

Based on the equilibrated dynamic trajectory, the binding free energy was calculated using the MM-PBSA method encoded in the AMBER 14.0 program. A total of 2000 snapshots from the trajectory were extracted every 50 ps, and the MM-PBSA calculation was performed on each snapshot using the MMPBSA.py.MPI module.

2.4. Fragment docking and direct coupling analysis (Fd-DCA)

Fd-DCA was a recently reported computational method that could accurately estimate druggable protein–protein interfaces [31]. We used this method to further validate the findings that were obtained by free energy decomposition.

2.5. General procedure for the synthesis of CMP5

Commercially available reagents were used without further purification. Organic solvents were evaporated with reduced pressure using a Buchi R-100 rotary evaporator. Reactions were monitored by TLC using Yantai Jiangyou (China) pre-coated GF254 silica gel plates. Silica gel column chromatography was performed on silica gel (200–300 mesh) from Qingdao Haiyang Chemical Plant (China). NMR spectra were measured on a Bruker Avance 600 spectrometer. Chemical shifts were expressed in δ (ppm) and coupling constants (J) in Hz using solvent signals as internal standards ($CDCl_3$, δ_H 7.27 ppm).

2.5.1. Synthesis of 1-(9-Ethyl-9H-carbazol-3-yl)-N-(pyridin-2-ylmethyl)methanamine (**CMP5**) [32]

A solution of *N*-ethyl-3-carbazolecarboxaldehyde (100 mg, 0.45 mmol), 2-(aminomethyl)-pyridine (49 mg, 0.45 mmol) and glacial acetic acid (1 drop, cat.) in anhydrous tetrahydrofuran (10 mL) was stirred at room temperature for 1 h. Sodium triacetoxyborohydride (95 mg, 0.45 mmol) was added in a single portion and the mixture stirred for a further 18 h. The reaction mixture was diluted with ethyl acetate and washed with a saturated aqueous solution of sodium hydrogen carbonate. The combined organic phase was washed with water, brine, and then dried over anhydrous magnesium sulfate, and the solvent was removed under vacuum. Purification by column chromatography (ethyl acetate) afforded **5** as an orange oil (88 mg, 0.28 mmol, 60%). **CMP5** was obtained by stirring **5** in HCl/Et_2O at room temperature for 1 h. ^1H NMR (600 MHz, $CDCl_3$) δ 8.60 (dd, J = 5.0, 1.6 Hz, 1H), 8.09–8.14 (m, 2H), 7.64 (td, J = 7.7, 1.7 Hz, 1H), 7.52–7.44 (m, 2H), 7.42–7.32 (m, 3H), 7.24 (t, J = 7.4 Hz, 1H), 7.17 (dd, J = 7.5, 5.0 Hz, 1H), 4.35 (q, J = 7.3 Hz, 2H), 4.06 (s, 2H),

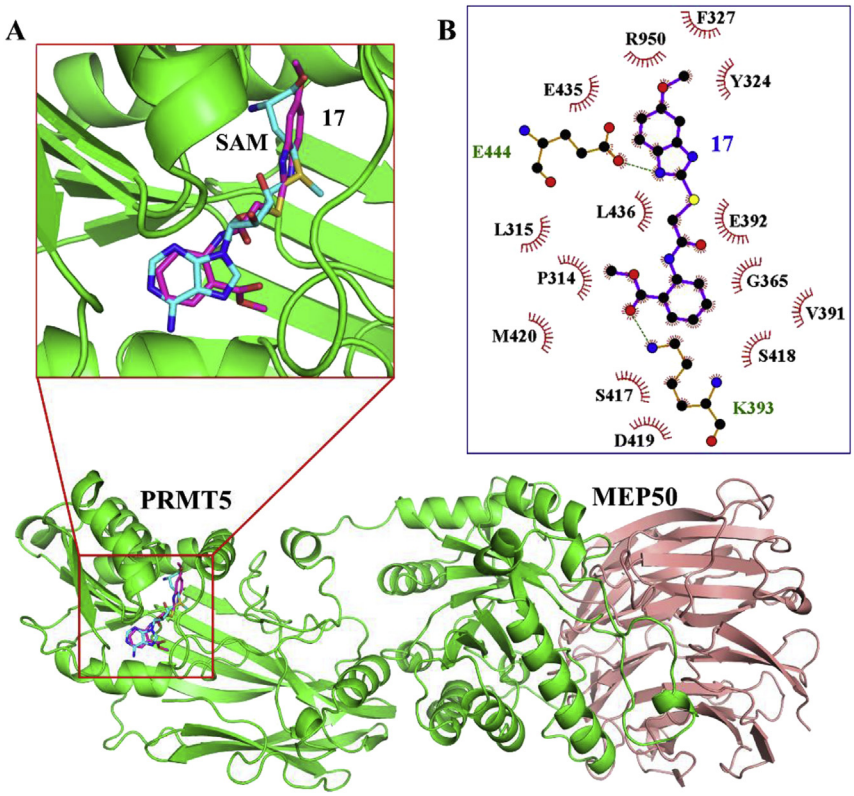

Fig. 1. (A) The binding mode of **17** with PRMT5. SAM was also displayed for comparison. PRMT5 and MEP50 were shown as cartoons, while **17** and SAM were shown as sticks. For clarity, the hydrogen atoms of **17** and SAM were not shown. (B) Hydrogen bonds and hydrophobic interactions between **17** and PRMT5. Hydrogen bonds are indicated by dashed lines, while hydrophobic contacts are represented by an arc with spokes radiating towards the ligand atoms. Molecular graphic figures were prepared with the LigPlot+ program.

Please cite this article in press as: K. Zhu, et al., Interaction assessments of the first S-adenosylmethionine competitive inhibitor and the essential interacting partner methylosome protein 50 with protein arginine methyltransferase 5 by combined computational methods, Biochemical and Biophysical Research Communications (2017), https://doi.org/10.1016/j.bbrc.2017.11.089

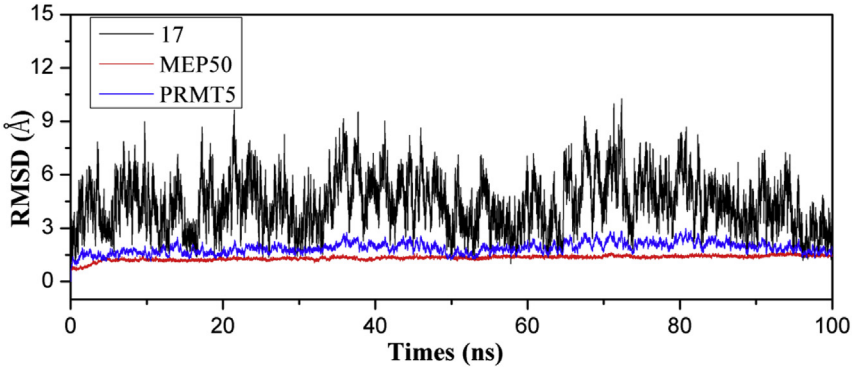

Fig. 2. Time dependencies of the weighted root-mean-square deviations (RMSD) for the backbone atoms of **17**, PRMT5 and MEP50 from their initial positions during the 100 ns simulation.

4.02 (s, 2H), 1.43 (t, J = 7.3 Hz, 3H). The ^{1}H NMR spectral data of **5** were in agreement with the literature data [32].

2.6. Direct inhibition activity of CMP5 against PRMT5 at enzymatic level assay

We followed the radioactive methylation assay method that we previously reported [14] to test the direct inhibition activity of **CMP5** against PRMT5 at enzymatic level.

3. Results

3.1. The predicted binding mode of 17 is similar to that of SAM

Molecular docking was used to gain the binding mode of **17** to PRMT5. As shown in Fig. 1A, **17** displayed binding mode similar to that of SAM. The detailed interactions between **17** and PRMT5 were shown in Fig. S1. To further validate the interaction, 100 ns MD simulation was performed on the inhibitor-enzyme (**17**-PRMT5:MEP50) complex model obtained by molecular docking. To examine the structural stability of the **17**-PRMT5:MEP50 complex model during MD simulations, the time evolution of weighted root-mean-square deviations (RMSDs) for backbone atoms of PRMT5:MEP50 protein and for heavy atoms of **17** from their initial positions (t = 0) were calculated. As illustrated in Fig. 2, RMSD values of **17**, PRMT5 and MEP50 were all steady during the simulation. For the simulated time span of 100 ns, **17** displayed general stability and confinement in the SAM binding pocket of PRMT5, in conformity with the conformation from the docking result, indicating that the **17**-PRMT5:MEP50 complex model is thermodynamically favored. During this simulation time window, no significant conformational change of the PRMT5:MEP50 surface had been observed.

By analyzing the MD trajectory, we found that **17** showed strong tendency to be localized in the SAM binding pocket of PRMT5. Two conserved hydrogen bonds formed between **17** and residues E444 and K393 were found, with occupancy rate of 91.63% and 61.37%, respectively. It is worthwhile to note that, two hydrogen bonds between **17** and residues Glu435 and Tyr334 (Fig. S1) were configured in the original **17**-PRMT5:MEP50 complex model obtained by molecular docking, whereas both occupancy rates were lower than 50% during the 100 ns MD simulation. This could rationalize the necessity of employing MD simulation to obtain the rational binding mode of small molecules. As illustrated in Fig. 1B and Fig. S2, besides the two residues involved in hydrogen bonding interaction, residues associated with hydrophobic interactions between **17** and PRMT5 formed a hydrophobic pocket. The corresponding occupancy rates of the hydrophobic interaction residues were shown in Table 1. In order to quantify the binding affinity between **17** and PRMT5:MEP50, MM-PBSA method encoded in the AMBER 14 program was used to calculate the binding free energy of the **17**-PRMT5:MEP50 complex. As shown in Table 2, **17** indeed showed potent binding affinity with PRMT5.

3.2. Previously reported PRMT5 inhibitor CMP5 did not show inhibitory activity against PRMT5 at enzymatic level

CMP5 was previously reported as a SAM binding site inhibitor of PRMT5, without being tested its direct inhibitoty activity at enzymatic level. As one purpose of this study is to summarize the interaction characteristic of SAM binding site inhibitors with

Table 1
PRMT5 residues involved in hydrophobic interactions with **17** during the simulation time and the corresponding occupancy rates. Only the occupancy rates above 50% were shown.

Residues	Occupancy rate
Pro314	74%
Leu315	54%
Tyr324	69%
Phe327	92%
Gly365	81%
Val391	79%
Glu392	75%
Lys393	93%
Ser417	50%
Ser418	80%
Asp419	66%
Met420	65%
Glu435	99%
Leu436	89%
Arg950	89%

Table 2
The binding free energy of **17**, SAM and MEP50 to PRMT5 calculated by the MM-PBSA method. All calculated values were given in kcal/mol. ΔG = ΔGgas + ΔGsolv. ΔGgas represents the binding free energy in vacuum while ΔGsolv represents the solvation free energy change.

	ΔGgas	ΔGsolv	ΔG
17	−96.98	69.71	−27.27
SAM	−317.82	260.48	−57.34
MEP50	−1907.37	1646.85	−260.52

Please cite this article in press as: K. Zhu, et al., Interaction assessments of the first S-adenosylmethionine competitive inhibitor and the essential interacting partner methylosome protein 50 with protein arginine methyltransferase 5 by combined computational methods, Biochemical and Biophysical Research Communications (2017), https://doi.org/10.1016/j.bbrc.2017.11.089

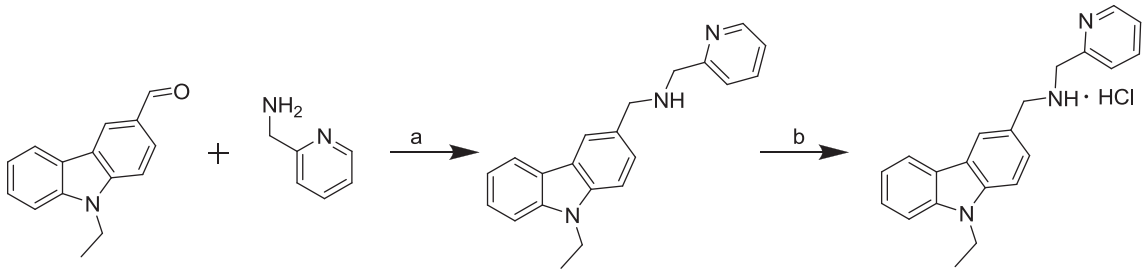

Scheme 1. Reagents and conditions: (a) $NaBH(OAc)_3$, AcOH, THF, rt, 18 h; (b) HCl/Et_2O, rt, 1 h.

PRMT5 by computational methods, we must know the IC_{50} of **CMP5** against PRMT5 at enzymatic level. Therefore, we synthesized this compound by following previously reported methods [32] (Scheme 1) and tested its inhibition against PRMT5 at enzymatic level according to the methods that we previously employed to screen PRMT5 inhibitors. The assay result showed that **CMP5** displayed barely inhibitory activity against PRMT5 at 50 μM with an inhibition rate of 7.8%. Based on the aforementioned observations, we believe that PRMT5 is not the direct target of **CMP5** despite the fact that it could block initiation and maintenance of B-cell transformation.

3.3. Key residues involved in interactions between PRMT5 and MEP50 were identified

MEP50, as the most important interacting partner of PRMT5, is essential for the catalytic activity of the latter. To probe the interactions between MEP50 and PRMT5, we constructed SAM-PRMT5:MEP50 and SAM-PRMT5 complex models, and then performed 100 ns MD simulations on the two models. Reliability of this two MD trajectories was confirmed by the stable RMSD values (Figs. S3 and S4) for backbone atoms of proteins (PRMT5 and MEP50) and for heavy atoms of SAM. In addition, we calculated the distance between the methyl carbon atom of SAM and the amino nitrogen atom of Arg3 residue of the SAM-PRMT5:MEP50 model during simulation, which represents a key factor of the methylation reaction catalyzed by PRMT5. As shown in Fig. S5, the distance fluctuated at ~3.5 Å, suitable for catalysis, which further supported the reliability of this model. Then based on the MD trajectory of SAM-PRMT5:MEP50 model, the binding free energy of SAM and MEP50 to PRMT5 were calculated by MM-PBSA method, respectively. As shown in Table 2, SAM displayed more potent binding affinity to PRMT5 compared with **17**, and the hydrogen bonds and hydrophobic interactions between SAM and PRMT5 were shown in Tables S1 and S2. As expected, the interaction between MEP50 and PRMT5 was very potent, with a binding free energy of −260.52 kcal/mol. To identify the regions of PRMT5 that involved in the binding with MEP50, the largest root-mean-square fluctuation (RMSF) values were calculated for the two models. Our results indicate that two regions (residues 54–74 and 158–180) of PRMT5 were responsible for the binding of MEP50 to PRMT5 (Fig. 3), because the residue fluctuations of the two regions significantly decreased in the SAM-PRMT5:MEP50 model compared with those in the SAM-PRMT5 model.

In order to further identify key residues that contribute most to the binding between PRMT5 and MEP50, energy decomposition calculation was performed. As we can see from Table 3, 22 residues of PRMT5 and 16 residues of MEP50 contributed to the binding between PRMT5 and MEP50. Then by further analyzing these residues, we found that a total of six residues (R49, R62, R91, R164, I168 and H271) of PRMT5 and three residues (R52, W54 and R164) of MEP50 contribute most to the binding free energy, with energy contribution < −5.0 kcal/mol (Fig. 4). This findings were in accordance with the Fd-DCA calculation results (Fig. S7).

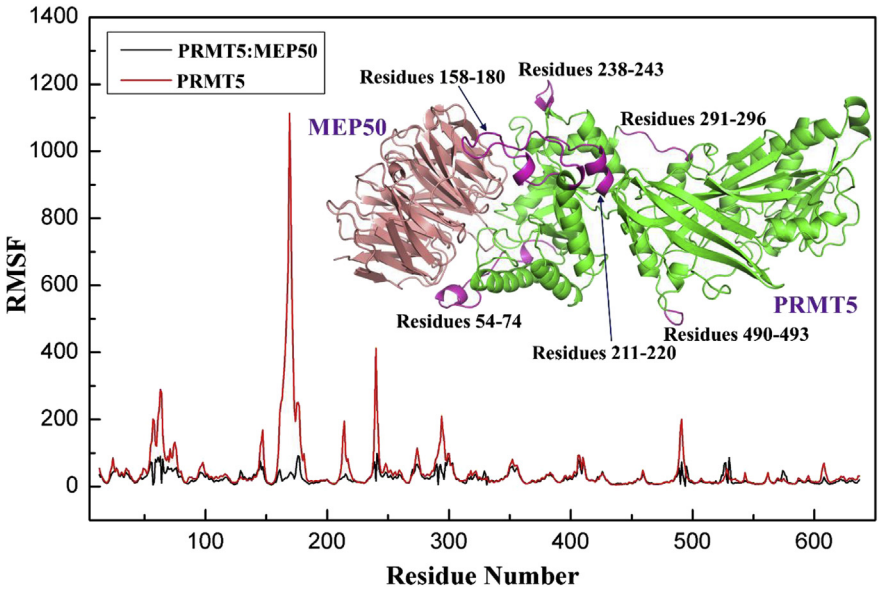

Fig. 3. Residue fluctuations of SAM-PRMT5:MEP50 and SAM-PRMT5 models over 100 ns simulations.

Please cite this article in press as: K. Zhu, et al., Interaction assessments of the first S-adenosylmethionine competitive inhibitor and the essential interacting partner methylosome protein 50 with protein arginine methyltransferase 5 by combined computational methods, Biochemical and Biophysical Research Communications (2017), https://doi.org/10.1016/j.bbrc.2017.11.089

Table 3
Decomposition of binding free energy ΔG into contributions from residues in PRMT5 and MEP50 binding surface. Only residues with contribution < −2 kcal/mol were shown. Values that are more negative indicate more contributions to substrate binding by the corresponding residues.

Residues number (PRMT5)	Energy contribution (kcal/mol)	Residues number (MEP50)	Energy contribution (kcal/mol)
Asn21	−4.52	Ser50	−2.08
Pro24	−4.39	Arg52	−8.97
Glu25	−2.50	Trp54	−8.88
His47	−4.97	Ile127	−2.80
Arg49	−17.38	Tyr163	−2.69
Phe50	−2.63	Arg164	−7.02
Lys51	−3.41	Ala167	−2.18
Pro58	−2.78	Glu188	−4.14
Arg62	−9.24	Lys201	−2.80
Arg68	−4.57	Ala203	−2.62
Arg91	−7.67	Ser204	−4.40
Lys95	−4.53	Gln205	−3.86
Val96	−2.06	Glu276	−4.34
Lys98	−2.38	Asp298	−2.02
Glu161	−2.82	Phe299	−3.14
Arg164	−6.57	Trp318	−2.48
Ile167	−3.84		
Ile168	−5.65		
Glu169	−4.72		
Asn170	−3.33		
Thr269	−3.57		
His271	−7.43		

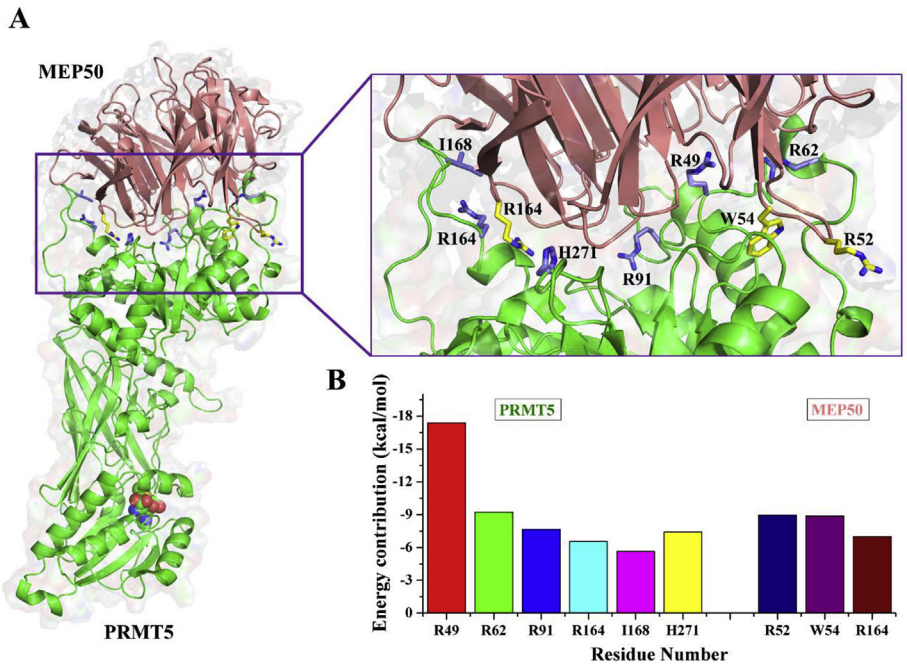

Fig. 4. Key residues that contributed most (with energy contribution < −5 kcal/mol) to the binding between MEP50 and PRMT5. (A) Identified residues were shown as sticks while PRMT5 and MEP50 were shown as cartoons. (B) Energy contributions of key residues of PRMT5 and MEP50 that contributed most to the binding.

4. Discussion

Acting as one of the most promising anticancer target in PRMT family, PRMT5 attracts more and more attention and considerable efforts have been made to discover inhibitors of PRMT5. With the purpose of providing clues to identify SAM binding site inhibitors of PRMT5, we conducted the current study. Up to now, **17** and **CMP5** were reported as SAM competitive inhibitors, but the direct inhibition activity of **CMP5** against PRMT5 at enzymatic level was not tested. Therefore, **CMP5** was synthesized and tested its direct inhibition against PRMT5 at enzymatic level. Our result showed that the IC_{50} of **CMP5** was above 50 μM, suggesting that PRMT5 was not the direct target of **CMP5**. Then, only the **17**-PRMT5:MEP50 model was constructed and assessed its binding characteristics to PRMT5. In addition, the interaction between PRMT5 and MEP50 was also investigated by combined computational methods, and nine key residues were identified to contribute most to the interaction. This finding is of great useful in designing mutant residue assay to modulate the catalytic activity of PRMT5 as well as in identifying new PRMT5 inhibitors.

Please cite this article in press as: K. Zhu, et al., Interaction assessments of the first S-adenosylmethionine competitive inhibitor and the essential interacting partner methylosome protein 50 with protein arginine methyltransferase 5 by combined computational methods, Biochemical and Biophysical Research Communications (2017), https://doi.org/10.1016/j.bbrc.2017.11.089

Acknowledgments

This work was supported by Natural Science Foundation of Shandong Province [No. ZR2017BH038, JQ201721], the Young Taishan Scholars Program [No. tsqn20161037], Shandong Talents Team Cultivation Plan of University Preponderant Discipline [No. 10027], the Natural Science Foundation of China [21672082], and Shandong Key Development Project [No. 2016GSF201209].

Abbreviations

PRMT5	Protein arginine methyltransferase 5
PRMT	Protein arginine methyltransferase
SAM	S-adenosylmethionine
MEP50	methylosome protein 50
MD	Molecular dynamics
MM-PBSA	Molecular mechanics/Poisson-Boltzmann surface area

Transparency document

Transparency document related to this article can be found online at https://doi.org/10.1016/j.bbrc.2017.11.089.

Appendix A. Supplementary data

Supplementary data related to this article can be found at https://doi.org/10.1016/j.bbrc.2017.11.089.

References

[1] J. Fuhrmann, K.W. Clancy, P.R. Thompson, Chemical biology of protein arginine modifications in epigenetic regulation, Chem. Rev. 115 (2015) 5413–5461.
[2] H. Hu, K. Qian, M.C. Ho, Y.G. Zheng, Small molecule inhibitors of protein arginine methyltransferases, Expert. Opin. Inv. Drug 25 (2016) 335–358.
[3] M.T. Bedford, S.G. Clarke, Protein arginine methylation in mammals: who, what, and why, Mol. Cell 33 (2009) 1–13.
[4] V. Karkhanis, Y.J. Hu, R.A. Baiocchi, A.N. Imbalzano, S. Sif, Versatility of PRMT5-induced methylation in growth control and development, Trends Biochem. Sci. 36 (2011) 633–641.
[5] Y. Yang, M.T. Bedford, Protein arginine methyltransferases and cancer, Nat. Rev. Cancer 13 (2013) 37–50.
[6] A. Di Lorenzo, M.T. Bedford, Histone arginine methylation, FEBS Lett. 585 (2011) 2024–2031.
[7] T.L. Branscombe, A. Frankel, J.H. Lee, J.R. Cook, Z. Yang, S. Pestka, S. Clarke, PRMT5 (Janus kinase-binding protein 1) catalyzes the formation of symmetric dimethylarginine residues in proteins, J. Biol. Chem. 276 (2001) 32971–32976.
[8] Y. Yang, A. Hadjikyriacou, Z. Xia, S. Gayatri, D. Kim, C. Zurita-Lopez, R. Kelly, A. Guo, W. Li, S.G. Clarke, M.T. Bedford, PRMT9 is a type II methyltransferase that methylates the splicing factor SAP145, Nat. Commun. 6 (2015) 6428.
[9] Y. Feng, R. Maity, J.P. Whitelegge, A. Hadjikyriacou, Z. Li, C. Zurita-Lopez, Q. Al-Hadid, A.T. Clark, M.T. Bedford, J.Y. Masson, S.G. Clarke, Mammalian protein arginine methyltransferase 7 (PRMT7) specifically targets RXR sites in lysine- and arginine-rich regions, J. Biol. Chem. 288 (2013) 37010–37025.
[10] S. Bandyopadhyay, D.P. Harris, G.N. Adams, G.E. Lause, A. McHugh, E.G. Tillmaand, A. Money, B. Willard, P.L. Fox, P.E. Dicorleto, HOXA9 methylation by PRMT5 is essential for endothelial cell expression of leukocyte adhesion molecules, Mol. Cell. Biol. 32 (2012) 1202–1213.
[11] D. Zakrzewicz, A. Zakrzewicz, K.T. Preissner, P. Markart, M. Wygrecka, Protein Arginine Methyltransferases (PRMTs): promising targets for the treatment of pulmonary disorders, Int. J. Mol. Sci. 13 (2012) 12383–12400.
[12] L. Alinari, K.V. Mahasenan, F. Yan, V. Karkhanis, J.H. Chung, E.M. Smith, C. Quinion, P.L. Smith, L. Kim, J.T. Patton, R. Lapalombella, B. Yu, Y. Wu, S. Roy, A. De Leo, S. Pileri, C. Agostinelli, L. Ayers, J.E. Bradner, S. Chen-Kiang, O. Elemento, T. Motiwala, S. Majumder, J.C. Byrd, S. Jacob, S. Sif, C. Li, R.A. Baiocchi, Selective inhibition of protein arginine methyltransferase 5 blocks initiation and maintenance of B-cell transformation, Blood 125 (2015) 2530–2543.
[13] I. Street, B. Monahan, H. Falk, E. Allan, Y. Bergman, P. Stupple, I. Holmes, A. Gregg, S. Charman, K. Lackovic, T. Peat, S. Walker, K. Lowes, W. Kersten, J. Alcindor, M. Chung, M. Parker, R. Foitzik, M. Camerino, M. Nikac, J. Grusovin, P. Pilling, S. Sonderegger, Y. Tan, Q. Zhao, D.J. Curtis, S.M. Jane, Selective inhibitors of arginine methyl transferase 5 (PRMT5) as a novel treatment for beta-thalassemia and sickle cell disease, Blood 120(21): 2129.
[14] R. Mao, J. Shao, K. Zhu, Y. Zhang, H. Ding, C. Zhang, Z. Shi, H. Jiang, D. Sun, W. Duan, C. Luo, Potent, selective, and cell active protein arginine methyltransferase 5 (PRMT5) inhibitor developed by structure-based virtual screening and hit optimization, J. Med. Chem. 60 (2017) 6289–6304.
[15] Y. Ye, B. Zhang, R. Mao, C. Zhang, Y. Wang, J. Xing, Y.C. Liu, X. Luo, H. Ding, Y. Yang, B. Zhou, H. Jiang, K. Chen, C. Luo, M. Zheng, Discovery and optimization of selective inhibitors of protein arginine methyltransferase 5 by docking-based virtual screening, Org. Biomol. Chem. 15 (2017) 3648–3661.
[16] S. Ji, S. Ma, W.J. Wang, S.Z. Huang, T.Q. Wang, R. Xiang, Y.G. Hu, Q. Chen, L.L. Li, S.Y. Yang, Discovery of selective protein arginine methyltransferase 5 inhibitors and biological evaluations, Chem. Biol. Drug Des. 89 (2017) 585–598.
[17] E. Chan-Penebre, K.G. Kuplast, C.R. Majer, P.A. Boriack-Sjodin, T.J. Wigle, L.D. Johnston, N. Rioux, M.J. Munchhof, L. Jin, S.L. Jacques, K.A. West, T. Lingaraj, K. Stickland, S.A. Ribich, A. Raimondi, M.P. Scott, N.J. Waters, R.M. Pollock, J.J. Smith, O. Barbash, M. Pappalardi, T.F. Ho, K. Nurse, K.P. Oza, K.T. Gallagher, R. Kruger, M.P. Moyer, R.A. Copeland, R. Chesworth, K.W. Duncan, A selective inhibitor of PRMT5 with in vivo and in vitro potency in MCL models, Nat. Chem. Biol. 11 (2015) 432–437.
[18] D. Smil, M.S. Eram, F. Li, S. Kennedy, M.M. Szewczyk, P.J. Brown, D. Barsyte-Lovejoy, C.H. Arrowsmith, M. Vedadi, M. Schapira, Discovery of a dual PRMT5-PRMT7 inhibitor, ACS Med. Chem. Lett. 6 (2015) 408–412.
[19] S. Antonysamy, Z. Bonday, R.M. Campbell, B. Doyle, Z. Druzina, T. Gheyi, B. Han, L.N. Jungheim, Y. Qian, C. Rauch, M. Russell, J.M. Sauder, S.R. Wasserman, K. Weichert, F.S. Willard, A. Zhang, S. Emtage, Crystal structure of the human PRMT5:MEP50 complex, Proc. Natl. Acad. Sci. U. S. A. 109 (2012) 17960–17965.
[20] Z.Q.C. Bonday, G. S.; Dahnke, K. R.; Grogan, M. J.; Hergueta, A. R.; Jamison, J. A.; Watson, B. M.; Woods, T. A., Preparation of 5'-substituted nucleoside analogs as antitumor agents, WO2016178870A1, (2016).
[21] T.B. Wu, D.; Beke, L.; Boeckx, A.; Diels, G. S. M.; Gilissen, R. A. H. J.; Lawson, E. C.; Pande, V.; Parade, M. C. B. C.; Schepens, W. B. G.; Thuring, J. W. J. F.; Viellevoye, M.; Sun, W.; Meerpoel, L., Preparation of 6-6 bicyclic aromatic ring substituted nucleoside analogs for use as PRMT5 inhibitors, WO2017032840A1, (2017).
[22] T.A. Halgren, R.B. Murphy, R.A. Friesner, H.S. Beard, L.L. Frye, W.T. Pollard, J.L. Banks, Glide: a new approach for rapid, accurate docking and scoring. 2. Enrichment factors in database screening, J. Med. Chem. 47 (2004) 1750–1759.
[23] R.A. Friesner, J.L. Banks, R.B. Murphy, T.A. Halgren, J.J. Klicic, D.T. Mainz, M.P. Repasky, E.H. Knoll, M. Shelley, J.K. Perry, D.E. Shaw, P. Francis, P.S. Shenkin, Glide: a new approach for rapid, accurate docking and scoring. 1. Method and assessment of docking accuracy, J. Med. Chem. 47 (2004) 1739–1749.
[24] J.C. Gordon, J.B. Myers, T. Folta, V. Shoja, L.S. Heath, A. Onufriev, H++: a server for estimating pKas and adding missing hydrogens to macromolecules, Nucleic Acids Res. 33 (2005) W368–W371.
[25] D.A. Case, T.E. Cheatham 3rd, T. Darden, H. Gohlke, R. Luo, K.M. Merz Jr., A. Onufriev, C. Simmerling, B. Wang, R.J. Woods, The Amber biomolecular simulation programs, J. Comput. Chem. 26 (2005) 1668–1688.
[26] J. Wang, R.M. Wolf, J.W. Caldwell, P.A. Kollman, D.A. Case, Development and testing of a general amber force field, J. Comput. Chem. 25 (2004) 1157–1174.
[27] J. Wang, W. Wang, P.A. Kollman, D.A. Case, Automatic atom type and bond type perception in molecular mechanical calculations, J. Mol. Graph. Model. 25 (2006) 247–260.
[28] J.P. Ryckaert, G. Ciccotti, H.J.C. Berendsen, Numerical-integration of cartesian equations of motion of a system with constraints - molecular-dynamics of N-alkanes, J. Comput. Phys. 23 (1977) 327–341.
[29] T. Darden, D. York, L. Pedersen, Particle Mesh Ewald - an N.Log(N) method for Ewald sums in large systems, J. Chem. Phys. 98 (1993) 10089–10092.
[30] H.J.C. Berendsen, J.P.M. Postma, W.F. Vangunsteren, A. Dinola, J.R. Haak, Molecular-dynamics with coupling to an external bath, J. Chem. Phys. 81 (1984) 3684–3690.
[31] F. Bai, F. Morcos, R.R. Cheng, H. Jiang, J.N. Onuchic, Elucidating the druggable interface of protein-protein interactions using fragment docking and coevolutionary analysis, Proc. Natl. Acad. Sci. U. S. A. 113 (2016) E8051–E8058.
[32] D. Rennison, S.M. Gueret, O. Laita, R.J. Bland, I.A. Sutherland, I.K. Boddy, M.A. Brimble, Substituted carbazoles - a new class of anthelmintic agent, Aust. J. Chem. 69 (2016) 1268–1276.

Please cite this article in press as: K. Zhu, et al., Interaction assessments of the first S-adenosylmethionine competitive inhibitor and the essential interacting partner methylosome protein 50 with protein arginine methyltransferase 5 by combined computational methods, Biochemical and Biophysical Research Communications (2017), https://doi.org/10.1016/j.bbrc.2017.11.089